Seismic force demand on ductile reinforced concrete shear walls subjected to western North American ground motions: Part 1 — parametric study

Yannick Boivin and Patrick Paultre

Abstract: A parametric study of regular ductile reinforced concrete (RC) cantilever walls designed with the 2010 National building code of Canada and the 2004 Canadian Standards Association (CSA) standard A23.3 for Vancouver is performed to investigate the influence of the following parameters on the higher mode amplification effects, and hence on the seismic force demand: number of storeys, fundamental lateral period (T), site class, wall aspect ratio, wall cross-section, and wall base flexural overstrength (γ_w). The study is based on inelastic time-history analyses performed with a multilayer beam model and a smeared membrane model accounting for inelastic shear–flexure–axial interaction. The main conclusions are that (*i*) T and γ_w are the studied parameters affecting the most dynamic shear amplification and seismic force demand, (*ii*) the 2004 CSA standard A23.3 capacity design methods are inadequate, and (*iii*) a single plastic hinge design may be inadequate and unsafe for regular ductile RC walls with $\gamma_w < 2.0$.

Key words: parametric study, 2004 CSA standard A23.3, ductile concrete cantilever wall, capacity design, higher mode amplification effects, seismic force demand.

Résumé : Une étude paramétrique de murs ductiles réguliers en béton armé dimensionnés avec le Code national du bâtiment 2010 du Canada et la norme CSA A23,3 2004 pour Vancouver est réalisée afin d'étudier l'influence des paramètres suivants sur les effets d'amplification des modes supérieurs, et donc sur la demande sismique en force : le nombre d'étages, la période fondamentale de vibration latérale (T), la classe du site, l'élancement du mur, la section du mur et la surcapacité flexionnelle à la base du mur (γ_w). L'étude est basée sur des analyses dynamiques inélastiques réalisées à l'aide d'une modélisation par poutres multi-couches et une modélisation par membranes considérant l'interaction inélastique force axiale–flexion–cisaillement. Les conclusions principales sont que (*i*) T et γ_w sont les paramètres étudiés ayant le plus d'influence sur l'amplification dynamique en cisaillement et la demande sismique en force, (*ii*) les méthodes de dimensionnement à la capacité de la norme CSA A23,3 2004 sont inadéquates et (*iii*) une conception à rotule plastique unique peut être inadéquate et non sécuritaire pour des murs ductiles réguliers en béton armé dont $\gamma_w < 2{,}0$.

Mots-clés : étude paramétrique, norme CSA A23,3 2004, mur ductile en béton armé, dimensionnement à la capacité, effets d'amplification des modes supérieurs, demande sismique en force.

1. Introduction

To produce economical seismic designs, the modern building codes allow reducing seismic design forces if the seismic force resisting system (SFRS) of a building is designed to develop an identified mechanism of inelastic lateral response. The capacity design aims to ensure that the inelastic mechanism develops as intended and no undesirable failure modes occur. Since the 1984 edition, this design approach is implemented in the Canadian Standards Association (CSA) standard A23.3 for seismic design of ductile reinforced concrete (RC) shear walls with the objectives of providing sufficient flexural strength to confine the inelastic mechanism to identified flexural plastic hinges and sufficient shear strength to ensure a flexure-governed inelastic lateral response of the walls. The implemented capacity design requirements intend to constrain the inelastic mechanism of a regular wall at the expected base plastic hinge. This design is referred to as single plastic hinge (SPH) design.

Despite the large improvements made to the seismic design provisions of the 2005 edition of the National building code of Canada (NBCC) (NRCC 2005) and the 2004 edition of the CSA standard A23.3 (A23.3-04) (CSA 2004), these codes can still produce inadequate and potentially risky seismic designs of regular multistorey ductile RC cantilever or coupled wall structures whose seismic force response is dominated by lateral modes of vibration higher than the fundamental lateral mode. The recent work of Boivin and Paultre (2010) shows that for such walls the capacity design shear envelope determined from these codes to prevent shear failure can largely

Received 14 November 2011. Revision accepted 4 April 2012. Published at www.nrcresearchpress.com/cjce on XX June 2012.

Y. Boivin and P. Paultre. Department of Civil Engineering, Université de Sherbrooke, Sherbrooke, QC J1K 2R1, Canada.

Corresponding author: Patrick Paultre (e-mail: Patrick.Paultre@usherbrooke.ca).

Written discussion of this article is welcomed and will be received by the Editor until 30 November 2012.

underestimate the shear force demand under design-level ground motions, even when the wall response is slightly inelastic. This underestimation results from a deficiency of these codes to account for dynamic amplification effects, in the elastic and inelastic regimes, due to higher lateral modes. Boivin and Paultre identified two sources for this underestimation: (*i*) the 2005 NBCC spectral accelerations underestimate the elastic responses of higher lateral modes of the walls because their traditional 5% damping overestimates actual damping (about 2% on average) and hence reduces the higher mode responses; and (*ii*) the capacity design methods prescribed by CSA standard A23.3-04 for shear strength design do not account for the dynamic amplification of shear forces due to inelastic effects of higher modes. No such underestimation problem in flexure was reported by Boivin and Paultre, likely because of the large flexural overstrength of the wall system studied by the authors. However, the capacity design method for flexural strength design prescribed by CSA standard A23.3-04 to prevent unintended plastic hinges above the base hinging region is not free from such a problem because its formulation based on amplified elastic forces is tributary of the analysis method, static or dynamic, used to derive these forces. The minor changes made to the seismic provisions of the 2010 NBCC (NRCC 2010) do not address these issues.

In this regard, this work proposes for CSA standard A23.3 new capacity design methods, considering higher mode amplification effects, for determining, for a SPH design, capacity design envelopes for flexural and shear strength design of regular ductile RC cantilever wall structures used as SFRS for multistorey buildings. This objective is achieved first by investigating from a parametric study the influence of various parameters on the higher mode amplification effects, and hence on the seismic force demand, in these walls, and second by deriving from the investigation results new capacity design methods for determining adequate capacity design shear and moment envelopes for such walls over their height. Note that the work focusses solely on cantilever walls because higher mode amplification effects are usually much more important in cantilever walls than in coupled walls.

This paper presents the first part of this work, that is, the parametric study. The paper is broken down into first a short literature review on higher mode amplification effects in RC walls to identify parameters that can have a significant influence on these effects, followed by an outline of the methodology adopted for the parametric study, and finally a presentation and a discussion on the results.

2. Review on higher mode effects in RC walls

The seismic force response of RC shear wall structures used as SFRS for multistorey buildings is generally dominated by the lateral modes of vibration higher than the fundamental lateral mode, on which is traditionally based the common static code procedure for seismic design. The predominating contribution of higher lateral modes in the elastic response of such walls produces moment and shear force demand profiles over the wall height significantly different from and larger (especially at the wall base for shear and at the upper storeys for flexure) than those resulting from the static code procedure. These well-known effects are associated to elastic effects of higher lateral modes. An additional dynamic effect occurs when the wall response changes from elastic to inelastic because the relative contribution of higher lateral modes, primarily that of the second mode, increases while the first-mode contribution satures and reduces with the first-mode period lengthening (Seneviratna and Krawinkler 1994; Priestley 2003; Sangarayakul and Warnitchai 2004). This dynamic amplification is associated to inelastic effects of higher lateral modes.

Research on higher mode amplification effects in RC walls has mainly focussed on the estimation of seismic shear forces in cantilever walls designed for a SPH at the base. The research has led to several relations for estimating seismic shear force demand on cantilever walls, particularly the base shear force. In most of these relations, the shear force corresponding to first-mode response at flexural capacity is increased by a dynamic amplification factor accounting for the elastic and inelastic effects of higher modes. In the following, a review of these dynamic factors is conducted to identify the parameters having a significant influence on the higher mode effects in cantilever walls and bring out the trends of their influence.

The pioneering work on higher mode effects in RC cantilever walls is that of Blakeley et al. (1975), which is based on inelastic dynamic analyses of isolated walls designed for a SPH at the base. The authors found that, at some instants of the response, the resultant lateral inertia force of a predominantly higher-mode response can be located much lower along the wall height than that of a first-mode response, producing a base shear increase and a base moment reduction. Moreover, they found that this base shear amplification increases with the fundamental lateral period of vibration, T_1, of the structure and the ground motion intensity, given the essentially elastic response of higher modes, and decreases with the flexural overstrength at the wall base. In addition, they highlighted the possibility of plastic hinge formation at levels above the base. The main outcome from this work is the well-known dynamic shear magnification factor for cantilever walls, ω_v, implemented in the New Zealand concrete design standard (NZS 2006) to magnify the static shear force corresponding to first-mode response at flexural capacity:

$$[1] \qquad \omega_v = \begin{cases} 0.9 + N/10 & N \leq 6 \\ 1.3 + N/30 \leq 1.8 & N > 6 \end{cases}$$

where N is the number of storeys of the building. This factor accounts for the elastic and inelastic effects of higher modes. Iqbal and Derecho (1980) proposed similar factors, based on T_1 this time, for shear and moment strength design.

Several works (Kabeyasawa and Ogata 1984; Aoyama 1987; Ghosh and Markevicius 1990) attempted to estimate the maximum seismic shear force V_{max} at the base of a SPH RC cantilever wall, isolated or part of a wall-frame structure, by adding to the wall base shear force corresponding to first-mode response at flexural capacity, V_{1y}, a force corresponding to higher mode responses, V_{hm}. All these works proposed a relation whose format is in essence the same and has shown to be in good agreement with experimental results (Eberhard and Sozen 1993). This relation can be expressed as follows:

$$[2] \qquad V_{max} = V_{1y} + V_{hm} = M_y/0.67H + D_m W A_g = \omega_{mv} V_{1y}$$

$$[3] \quad \omega_{mv} = 1 + D_m W A_g / V_{1y}$$

where ω_{mv} is a dynamic base shear amplification factor, M_y is the wall bending strength at the base determined from an inverted triangular force distribution over the entire height H of the wall, W is the total weight of the structure, A_g is a peak acceleration coefficient, expressed as a ratio of gravitational acceleration, taken as either the peak acceleration or an effective peak acceleration of the input ground motion, and D_m is a coefficient that for some is constant and equal to 0.25 (Ghosh and Markevicius 1990), and for others increases with the number of storeys (N) of the structure (Kabeyasawa and Ogata 1984; Aoyama 1987) and with the design displacement ductility ratio, μ_Δ (Seneviratna and Krawinkler 1994). For $N \geq 30$, Seneviratna and Krawinkler (1994) observed that D_m becomes independent from the ductility ratio and converges toward a value of about 0.34, as found by Aoyama (1987). The dependence of ω_{mv} (eq. [3]) on N is in line with that of ω_v (eq. [1]). However, ω_{mv} directly captures more parameters having an influence on higher mode effects than ω_v. This deficiency of ω_v in capturing causative parameters can result in significant underestimations of dynamic shear amplification in walls (Keintzel 1990; Seneviratna and Krawinkler 1994; Priestley and Amaris 2003).

From inelastic dynamic analyses of isolated SPH RC cantilever walls designed from a direct displacement-based design (DDBD) method, Priestley (2003) derived the following dynamic base shear amplification factor, ω_v^*, which aims to amplify the base shear determined with the DDBD method and also attempts to fix the underestimation issue of ω_v (eq. [1]):

$$[4] \quad \omega_v^* = 1 + B_T \mu_\Delta / \phi_o$$

$$[5] \quad B_T = 0.067 + 0.4(T_1 - 0.5) \leq 1.15 \quad (T_1 \geq 0.5\,\text{s})$$

where ϕ_o is the flexural overstrength factor at the wall base. Figure 1 illustrates eq. [4] for $\mu_\Delta = 5.6$ and four ϕ_o values, and compares it with eq. [1]. Figure 1 shows a considerable influence of ϕ_o on dynamic base shear amplification and a large difference between the two relations, in part because of the different design methods to which they are associated. A comparison between eqs. [4] and [3] shows similarities, knowing that D_m in some extent depends on T_1 and that V_{1y} can be expressed as $\phi_o V_{1e}/\mu_\Delta$ where V_{1e} is the elastic base shear force associated to first lateral mode.

For RC walls designed for high ductility, the 2004 edition of the Eurocode 8 (EC8) (CEN 2004) requires that the design shear force diagram determined from linear analysis be amplified by the following dynamic shear amplification factor, ε, which is based on the formula proposed by Keintzel (1990):

$$[6] \quad \varepsilon = q\sqrt{\left(\frac{\gamma_{Rd}}{q} \cdot \frac{M_{Rd}}{M_{Ed}}\right)^2 + 0.1\left(\frac{S_e(T_c)}{S_e(T_1)}\right)^2}$$

with $1.5 \leq \varepsilon \leq q$, where q is the behavior factor (equivalent to μ_Δ) used for design, M_{Rd} is the design flexural resistance at the wall base, M_{Ed} is the design bending moment at the wall base, γ_{Rd} is the factor to account for overstrength due to strain hardening of the reinforcement (may be taken as 1.2),

Fig. 1. Comparison between the dynamic shear amplification factors ω_v (eq. [1]), ω_v^* (eq. [4]), and ε^* (eq. [7]) for μ_Δ ($\equiv q$) = 5.6 and assuming $T_1 = 0.1N$.

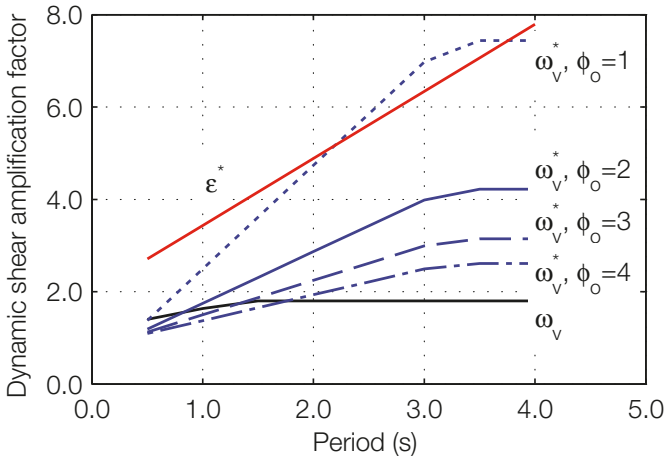

T_1 is the fundamental lateral period of the structure, T_c is the upper limit period of the constant spectral acceleration region of the spectrum and $S_e(T)$ is the ordinate of the elastic acceleration response spectrum at period T. Equation [6] was derived considering only the first two lateral vibration modes. The first term within the square root corresponds to the shear force likely to develop at flexural capacity under a first-mode response, while the second term corresponds to the shear increase due to higher mode effects. Note that, unlike CSA standard A23.3-04, which is silent on dynamic shear amplification in moderately ductile (MD) walls, the 2004 EC8 recommends $\varepsilon = 1.5$ for these walls. Various works (Linde 1998; Priestley and Amaris 2003; Rutenberg and Nsieri 2006) indicated that eq. [6] can significantly overestimate the dynamic base shear amplification in short-period ductile walls while underestimating it in long-period ones. In an attempt to fix that problem, Rutenberg and Nsieri (2006) proposed the following formulas for the 2004 EC8 for determining the seismic design base shear force, V_{db}, for ductile walls:

$$[7] \quad V_{db} = \varepsilon^* V_{by} = [0.75 + 0.22(T_1 + q + T_1 q)]V_{by}$$

$$[8] \quad V_{by} = \frac{M_y}{(2/3)H[1 + (1/2N)]}$$

where ε^* is a dynamic base shear amplification factor. Equation [7] is based on the observation that dynamic amplification of the base shear force increases quite linearly with T_1 and q. The ε^* factor is compared to eqs. [1] and [4] in Fig. 1 for $q = 5.6$.

Since the 2005 edition, the NBCC has introduced a new factor, M_v, in the calculation of the code-specified base shear force to account explicitly for the dynamic magnification of base shear due to elastic effects of higher modes. Table 1 gives the M_v values specified in the 2010 NBCC for cantilever walls. A ratio $S_a(0.2)/S_a(2.0) < 8.0$ is typical for the western Canadian regions, where earthquake ground motions have primarily a low frequency content, and a ratio $S_a(0.2)/S_a(2.0) \geq 8.0$ is typical for the eastern Canadian regions, where ground motions have principally a high frequency content. Once again, Table 1 shows, as eqs. [3] and [6], that, in addition to the fundamental

Table 1. Values specified in the 2010 NBCC for cantilever walls of the factor M_v to account for higher mode effects on base shear.

$S_a(0.2)/S_a(2.0)$	$T_a \leq 1.0$	$T_a = 2.0$	$T_a \geq 4.0$
<8.0	1.0	1.2	1.6
≥8.0	1.0	2.2	3.0

lateral period of the building (T_a), the input earthquake motion, and hence the seismic zone, has an influence on higher mode effects, such as suggested also by Filiatrault et al. (1994) for selecting their proposed shear reduction factor.

Based on the previous review on dynamic shear amplification factors, it can be concluded that the parameters most affecting the higher mode amplification effects in isolated RC cantilever walls are the fundamental lateral period (T_1) of the structure, and (or) the number of storeys (N), the design displacement ductility ratio (μ_Δ), the flexural overstrength at the wall base, and the ground motion intensity and frequency content, which implies the seismic zone which is characterized by its seismic hazard and site conditions. From all reviewed relations of dynamic shear amplification factor, eq. [3] appears the most appropriate to directly capture the main parameters affecting higher mode effects.

It is important to point out, however, that the above observations and relations for estimating dynamic shear amplification were derived from two-dimensional (2D) inelastic time-history analyses (ITHAs) performed with generally lumped plasticity beam elements where flexural deformation was modelled with bilinear hysteresis rules and shear deformation was modelled linearly elastic or with a nonlinear shear spring uncoupled from flexural and axial deformations. This simple modeling tends to largely overestimate shear predictions because important nonlinear physical phenomena, such as cracking, shear–flexure–axial interaction, and strength decay, that occur in actual laterally deformed RC walls are not taken into account. Moreover, such modeling could not capture the inelastic shear deformation differences between different wall cross-sections. In addition, the ITHAs were often carried out with strong historical ground motions of the western US that are not necessarily representative of the magnitude–distance ranges and tectonic environment that cause the seismic hazard of the main Canadian seismic regions for the design probability level. These important modeling deficiencies and input earthquake differences highlight the limitations of the presented observations and relations. This indicates the need for further investigation on the parameters influencing higher mode effects in isolated RC walls and for more sophisticated and representative simulations to get realistic estimates for Canadian regions.

It is also important to add that the list of parameters influencing the higher mode amplification effects in RC shear wall systems is not limited to those affecting isolated cantilever walls. System-related parameters, such as the beam-to-wall strength ratio in coupled walls (Munshi and Ghosh 2000), the sequence of hinge formation (Rutenberg and Nsieri 2006), and the relative inelastic shear deformation (Adebar and Rad 2007) between the walls composing a wall system, and the frame-to-wall stiffness ratio in dual systems (Rutenberg and Nsieri 2010), can also play a significant role on dynamic shear amplification. However, these parameters are not addressed in this paper.

3. Parametric study methodology

The parametric study aims to investigate the influence of various parameters on the higher mode amplification effects and hence on the seismic force demand on regular ductile RC cantilever walls. In this regard and based on the outcomes from the previous review, the methodology adopted in this work for the parametric study is as follows:

1. Selecting the parameters to be studied and assigning them a value range;
2. Designing and detailing for seismic forces each studied wall case with the 2010 NBCC and CSA standard A23.3-04 to meet the parameter values associated to that case;
3. Modeling and simulating numerically the inelastic seismic response of each studied case using two different modeling approaches, a simple one and a more realistic one;

Each stage is detailed in the following sections.

3.1. Studied parameters

From the parameters identified in section 2, the following were considered for the parametric study: number of storeys (N), fundamental lateral period (T), design displacement ductility ratio (μ_Δ), flexural overstrength at the wall base (γ_w), wall aspect ratio (A_r), wall cross-section (WCS), seismic zone, and site class (SC). The μ_Δ ratio and the seismic zone are the only two parameters fixed for the study. In the 2010 NBCC, the μ_Δ ratio corresponds to the product of the ductility-related and overstrength-related force reduction factors R_d and R_o, respectively, using the equal displacement assumption. For the ductile RC cantilever walls studied, the product $R_dR_o = 3.5 \times 1.6 = 5.6$. The seismicity of the city of Vancouver located on the Canadian West coast was selected for the study because this city has the highest urban seismic risk in Canada. Its high seismic hazard is representative of that of western Canadian cities and ductile RC walls are the preferred SFRS in this region. Figure 2 shows the 2010 NBCC design spectra for Vancouver for different site classes. Although the earthquake ground motions of the West coast have typically a lower high frequency content than those of eastern Canada, their motion intensity is in general much higher. Consequently, this gives a better control on flexural overstrength (γ_w) because seismic design is further governed by the design forces than by the required minimum reinforcement.

Table 2 gives the values considered for the studied varying parameters. The N values range from 5 to 40. For each N value, two T values were selected. Their selection is based on in situ measurements, shown in Fig. 3, of fundamental lateral periods of multistorey RC wall buildings. Using a mean storey height of 3.5 m, Fig. 3 shows that most of these measurements are within the range defined by T_a, the empirical fundamental period specified by the 2010 NBCC for wall buildings, and $2T_a$, the upper bound specified by the NBCC for seismic design of such structures. The selected T values are approximately equal to or within these limits and range from 0.5 s to 4.0 s, which is the minimum period of the constant acceleration region of the design spectra (see Fig. 2). Four different WCSs were considered: rectangular (RT),

Fig. 2. 2010 NBCC (5% damped) design spectra for Vancouver for different site classes (A: hard rock; B: rock; C: very dense soil and soft rock; D: stiff soil; E: soft soil).

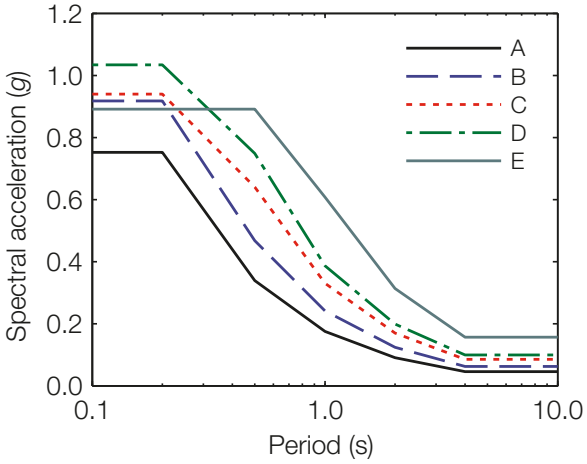

barbell-shaped (BB) and two I-shaped ones (I1 and H1), as illustrated in Fig. 4. For all studied cases, WCSs were bent about their strong axis. For a given N, a typical WCS was used except for $N = 20$ where the influence of the four different WCSs on the wall response was studied. In the elastic regime, for a given T, changing A_r does not affect the higher mode amplification effects because the latter are controlled by T. In the inelastic regime, however, the increase of higher mode contribution as T lengthens because of base yielding may likely result into larger dynamic shear amplifications for slender walls. The selected A_r values were obtained by changing the wall length (l_w) and by keeping constant the storey height, which is 3.5 m (3.0 m for three cases). This change results in different plastic hinge heights at the wall base as this height is assumed proportional to l_w. The flexural overstrength at the wall base, γ_w, is calculated as the ratio of the nominal moment resistance (M_n) and the design moment (M_f) at the wall base. As suggested by eq. [4] ($\phi_o \equiv \gamma_w$), γ_w reduces μ_Δ resulting in an effective μ_Δ, which provides a better estimate of the expected displacement ductility demand on a cantilever wall and hence of the likely dynamic amplification levels. Larger the γ_w, the lower should be the dynamic shear amplification in the inelastic regime, as shown in Fig. 1. The considered γ_w values range from 1.3 to 4.0, where 1.3 is the minimum value specified by CSA standard A23.3-04 for seismic design of wall structures and 4.0 approximates the theoretical overstrength limit before shear strength design of ductile walls is controlled by the elastic shear forces, which is $5.6/1.3 \approx 4.3$. As indicated in Table 2, four of the six site classes (SCs) defined in the 2010 NBCC were considered for the study. As shown in Fig. 2, the design spectra associated to the selected site classes enable to account for the possible soil amplification effects, excluding those associated to the unclassified site class F (other soils). The site class effects were studied only for $N \leq 10$ because soil amplification effects generally reduce with increasing T, assuming a soil, even a soft one, largely stiffer than the structure. From all selected parameter values, it results a total of 59 different wall cases, considering that a single SC was used when varying the γ_w values for a given N-T pair and vice versa.

3.2. Seismic design and detailing

For seismic design, each studied wall case was modelled as a fixed-base isolated wall meshed with linear beam elements. For a given T value, the total mass of the system was calculated using the Rayleigh period formula for a uniformly laterally loaded cantilever wall with considerations for shear deformation and for the mass idealization difference between the uniformly distributed mass assumed by the formula and the lumped mass adopted for modeling. Seismic design forces were obtained from the modal response spectrum method prescribed by the 2010 NBCC, with the exception that the design base shear force, V_d, was always that resulting from the modal superposition and the force reduction with R_dR_o (NBCC building importance factor, $I_E = 1$). In other words, the NBCC limitations about V_d were omitted as well as the NBCC requirements about accidental torsion. In all cases, the first five lateral mode responses were superposed with the SRSS (square root of the sum of the squares) method, ensuring a participation of at least 90% of the total mass. Concrete cracking was accounted for by using the effective section properties recommended by CSA standard A23.3-04, assuming an axial compressive force at the wall base, P_b, of $0.1f'_cA_g$, where f'_c is the specified concrete compressive strength and A_g is the gross cross-section area of the wall. The resulting effective properties equal to 70% of the gross properties. The specified material properties used for design are $f'_c = 30$ MPa and $f_y = 400$ MPa for steel yield strength. Typical wall thicknesses varying between 400 mm and 700 mm were used. The anticipated overall drifts for all studied cases are lower than 1.0%.

A capacity design was performed for each wall case according to CSA standard A23.3-04 to constrain the plastic mechanism at the wall base and prevent shear failure. As required, the capacity design shear envelope, V_{cap}, is the greater of (*i*) the shear corresponding to the development of the probable moment capacity of the wall base, which is determined as recommended in the *Explanatory notes on CSA standard A23.3-04* (CAC 2006), that is

$$[9] \qquad V_p = V_f\left(\frac{M_p}{M_f}\right)_{base}$$

where V_f is the design shear force, M_f is the design moment at the wall base, both determined from the modal response spectrum method, and M_p is the probable moment resistance at the wall base calculated with the specified concrete compressive strength f'_c and an equivalent steel yield stress of $1.25\,f_y$; and (*ii*) the shear, V_{ah}, corresponding to the development of the factored moment resistance just above the base hinge zone; but is not taken greater than the shear force limit, V_{limit}, which is determined from the elastic shear forces obtained from the modal superposition and reduced with $R_dR_o = 1.3$. Note that, above the hinge zone, V_{ah} was generally slightly larger than V_p, but never by more than 10%. Also, as expected, for all wall cases with $\gamma_w = 4.0$, V_{limit} controls the design and is less than V_p by no more than 10%. See Boivin and Paultre (2012) for more details on the required capacity design envelopes. The walls were reinforced in accordance with CSA standard A23.3-04, which means that reinforcement was set within the required minimum and maximum reinforcement limits. Moreover, curtailments of

Table 2. Varying parameter values for the parametric study.

N	T	WCS	A_r	γ_w	SC
5	0.5	RT	3.5	1.3, 2.0, 3.0, 4.0	A, C, D, E
	1.0	RT	5.833	1.3, 2.0, 3.0, 4.0	A, C, D, E
10	1.0	RT	3.5	2.0	A, C, D, E
		RT	4.375	2.0	C
		RT	5.833	1.3, 2.0, 3.0, 4.0	C
	1.5	RT	4.375	2.0	C
		RT	5.833	1.3, 2.0, 3.0, 4.0	A, C, D, E
		RT	8.75	2.0	C
15	1.0	BB	4.375	1.3, 2.0, 3.0, 4.0	D
	2.0	BB	7.0	1.3, 2.0, 3.0, 4.0	D
20	1.5	I1	7.0	2.0	D
	2.0	RT	7.0	2.0	D
		BB	7.0	1.3, 2.0, 3.0, 4.0	D
		I1	7.0	2.0	D
		H1	7.0	2.0	D
		I1	10.0	2.0	D
30	2.0	I1	8.57	2.0	D
	3.0	I1	10.0	1.3, 2.0, 3.0, 4.0	D
40	3.0	I1	10.0	2.0	D
	4.0	I1	11.67	1.3, 2.0, 3.0, 4.0	D

Fig. 3. Measured fundamental lateral periods vs. number of storeys of RC wall buildings compared to 2010 NBCC empirical period T_a (measurements are from Goel and Chopra 1998; Lee et al. 2000; Ventura et al. 2005; Kim et al. 2009; and Gilles 2010).

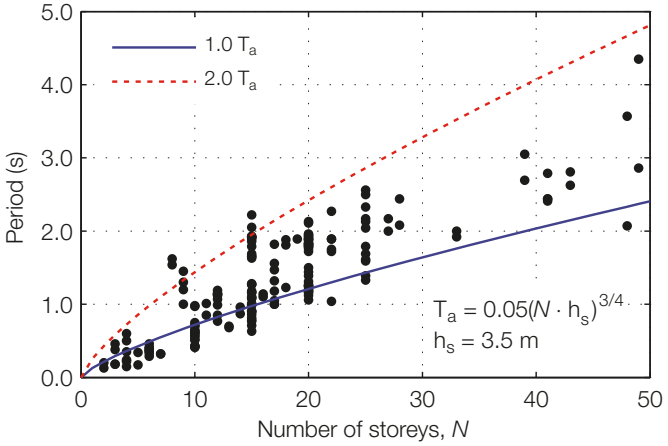

vertical reinforcement along the wall height were such that the wall flexural strength reduction between two adjacent storeys did not exceed between 20% and 10% for short and long-period walls, respectively. Preliminary analyses showed that, in some cases, larger strength reductions could produce at the upper storeys, as T increased, an unintended plastic hinge at the storey just above the reinforcement curtailment even if the flexural strength was greater than the capacity design envelope. Each wall was axially loaded by a static compression force reducing linearly from the base to the top, with a base axial force $P_b = 0.1f'_cA_g$, which is typical in actual multistorey RC walls. It is important to note that variations in the material properties or in the base axial compression force have negligible effects on the wall response in comparison with variations in the input earthquake. Therefore, f_y and P_b values were sometimes reasonably modified from their nominal value to meet the

Fig. 4. Wall cross-sections (WCSs) studied.

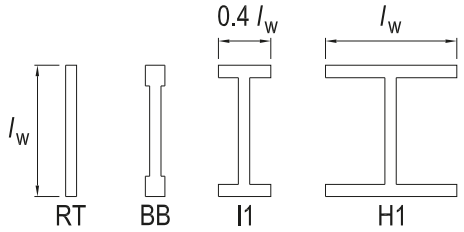

selected γ_w values. To that end, vertical reinforcement was also set slightly outside the prescribed reinforcement limits in some cases.

3.3. Modeling for inelastic seismic analysis

The simulation of the inelastic seismic response of each studied wall case was performed with the ITHA using the constant acceleration Newmark method for time integration. Each wall case was modelled as a fixed-base isolated cantilever wall. This modeling assumes that (*i*) the foundation moment resistance is such that the plastic mechanism forms in the wall only, (*ii*) there is no rocking of the foundation, and (*iii*) the soil–structure interaction can be neglected because the soil is largely stiffer than the structure. Note that foundation rocking is now allowed by the NBCC since the 2005 edition. This can significantly reduce the seismic force demand on a wall (Filiatrault et al. 1992).

3.3.1. Structural models

Two 2D modeling approaches were adopted for simulating the inelastic seismic response of each studied wall case. For the first approach, the finite element analysis program VecTor2 (VT2) (Wong and Vecchio 2002) was used. This specialized program enables the simulation at global and local levels of the nonlinear static and dynamic behaviors of RC structures from 4-node, smeared material-based membrane elements formulated from the modified compression field

Table 3. Selected VT2 concrete and steel constitutive laws.

Material	Constitutive law	Modelled response
Concrete	Popovics (NSC)	Compression pre-peak
	Modified Park-Kent	Compression post-peak
	Kupfer-Richart	Confined strength
	Palermo	Hysteretic response with strength decay
	Modified Bentz	Tension stiffening
Steel	Seckin (trilinear)	Hysteretic response with Bauschinger effect

Note: NSC, normal strength concrete.

theory and the disturbed stress field model (Vecchio 2000). With this formulation, reinforcement is assigned as a property to the membrane element and then smeared with concrete properties. This element formulation enables to account for inelastic shear deformation and shear–flexure–axial interaction. The VT2 constitutive laws selected to model the material responses of concrete and reinforcement steel are given in Table 3. The material properties were used at their specified value (nominal). The default laws of all other material responses modelled in VT2 were used for analysis as well as the default values of analysis parameters. Also P-delta effects were taken into account. The mass storey used for seismic design was lumped at each floor level, as illustrated in Fig. 5. The slab membrane effect at each floor level was modelled with linear elastic bar elements, as shown in Fig. 5, assuming an effective width of 1 m and a thickness of 200 mm. Other works have shown the reliability of VT2 to adequately simulate, with very similar modeling considerations and within the limits of similar design ductilities, cyclic and dynamic test responses of RC wall specimens designed with CSA standard A23.3-04 (Ghorbanirenani 2010). For the second modeling approach, the open-source software framework OpenSees (OS) (version 2.1.0) (Mazzoni et al. 2006) was used. In this approach, the wall structure was modelled using force-based multilayer beam–column elements with a mesh of one element per storey, and the mass storey was lumped at each floor level, as shown in Fig. 5. The hysteretic responses of concrete and reinforcement steel were modelled with the OS uniaxial material laws Concrete03 and Steel02, respectively. The strain hardening and the Bauschinger effect of reinforcement steel were taken into account. The backbone curves in compression and tension of the concrete law were represented with the modified Park-Kent model to account for confinement effects and the modified Bentz model (Vecchio 2000) to account for tension stiffening, respectively. The material properties were the same as those used for VT2. The wall shear deformation was modelled linearly elastic considering the effective shear area of the wall cross-section. This shear model was aggregated to the element formulation. It results in a shear deformation uncoupled from flexural and axial deformations. This modeling is a common simplification and its selection aims to assess the overestimation level it produces on shear response of ductile walls. The P-delta effects were modelled with a corotational transformation. The number of integration points (NIP) for each element was initially set to 5 for accuracy but the in-house Tcl (Tool command language) program developed for parametric analysis with OS automatically reduced

Fig. 5. Structural wall models for ITHA with OpenSees and VecTor2.

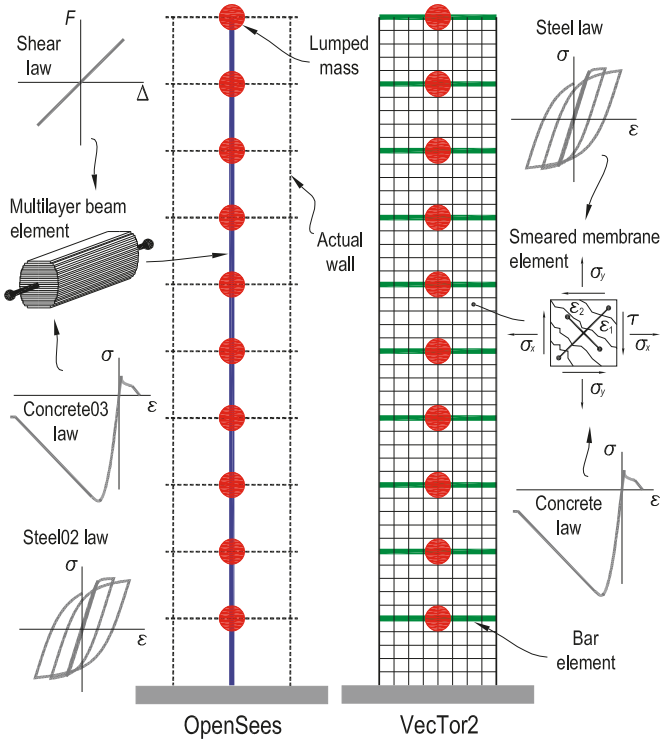

the NIP gradually up to 3 if convergence failed. This Tcl program also automatically changed within the analysis the nonlinear solution algorithm if convergence failure occurred. Preliminary analyses showed very good agreements between the dynamic deformation and force responses obtained from the VT2 simulations and those obtained from the OS simulations, apart from the OS peak responses being generally larger.

3.3.2. Damping model

The damping model used for ITHA with VT2 and OS is the initial stiffness-based Rayleigh damping because this is the sole damping model implemented in VT2. To avoid possible problems of spurious damping forces, and hence of force equilibrium, due to high damping in the high modes resulting from this model (Crisp 1980), Rayleigh damping was specified at the first mode and at the mode number equal to N, which is the last mode, ensuring that the highest modes of the structure remain sub-critically damped throughout the response. For seismic analysis of multi-degree-of-freedom building structures with $T > 0.5$ s, Léger and Dussault (1992) recommended Rayleigh damping and showed that the influence of the selected Rayleigh damping formulation is not so significant on the seismic response and becomes negligible for structures with $T > 1.5$ s. This suggests that the Rayleigh damping model used in this project does not limit the reach of the obtained results since the selected T values range from 0.5 s to 4.0 s. As damping is intended to model the intrinsic damping of buildings prior to concrete cracking, a modal damping ratio of 2% of critical was assigned to the first and last modes. This modal damping value is a typical mean value for multistorey RC wall buildings, though intrinsic damping of buildings is highly scattered (CTBUH 2008; Gilles 2010).

3.3.3. Input earthquakes

Atkinson (2009) generated synthetic earthquake time histories that may be used to match the 2005 NBCC uniform hazard spectra (UHS) for eastern and western Canadian regions and for site classes A, C, D, and E. These UHS correspond to a 2500 year return period earthquake event. For the western Canadian region and a given site class, Atkinson simulated 45 statistically independent records for each of the following magnitude-distance scenarios associated to crustal and in-slab earthquake events: M 6.5 at 10–15 km, M 6.5 at 20–30 km, M 7.5 at 15–25 km, and M 7.5 at 50–100 km. The M 6.5 and M 7.5 records correspond to short and long duration events, respectively. Since the 2005 and 2010 NBCC UHS for Vancouver are the same, 10 of these records were selected for each scenario of a site class and matched, as recommended by Atkinson, to the design spectra, resulting in 40 UHS-compatible records per site class. Note that the records were matched over period ranges specific to scenarios and not over the whole period range of a spectrum. Each record was used as a horizontal seismic excitation only. The constant time step of the records is either 0.002 s or 0.005 s.

It is relevant to note that the selected records were matched to the 5% damped design UHS, as recommended by the 2010 NBCC for design purposes, but were used for the seismic analysis of the studied structures with 2% Rayleigh damping. Matching with 2% damped UHS might have been more appropriate for the few studied cases where lateral deformations were expected to remain elastic. For the other cases, however, inelastic deformations add hysteretic damping to the initial damping, producing a total equivalent damping that may significantly exceed 5% of critical when deformations occur at yielding and beyond (Newmark and Hall 1982).

3.3.4. Inelastic time-history analysis

The selected 59 wall cases, with 40 records per case, and 2 modeling approaches resulted in a total of 4720 analyses. Because of the considerable number of analyses and the large analysis runtime and large amount of output data generated by VT2, the analyses were carried out with the 576-node parallel supercomputer of the University of Sherbrooke, producing more than 6 Tb of output data. To process this data, MATLAB stand-alone programs were developed and automatically executed after each analysis through a procedure script.

4. Dynamic analysis results

All predicted demands for a given wall case presented in this section are the means obtained from 40 ground motions. The dynamic shear amplification at a given storey is calculated as the ratio of the mean predicted storey shear force demand to V_p (eq. [9]). The dynamic shear amplification is calculated at the wall base and as the average value over all storeys (AOS). In addition to these response parameters, the predicted moment, storey shear force, and curvature ductility (μ_ϕ) demands over the wall height are presented. For clarity purposes, the presented curves of curvature ductility demand are envelopes of the maximum curvature ductility of each storey (which always occurs at the storey base for the studied walls), and hence are smoothed mean distributions of the curvature ductility demand along the wall height. The moment and storey shear force demands are normalized relative to the nominal base moment resistance ($M_{n\ base}$) and the predicted base shear force demand (V_{base}), respectively. It is noted that curvature ductility is only predicted with OS by estimating the global yield curvature of a wall section from a trilinear idealization of its monotonic moment–curvature response. VT2 does not output curvature which is not simple to determine because plane sections do not remain plane due to inelastic shear deformation. Nevertheless, the OS curvature predictions are reasonable estimates because OS generally predicted slightly more flexural yielding than VT2. Note that it was observed that the complete formation of a plastic hinge is associated to a rapid increase of the curvature ductility and that this formation occurs when $\mu_\phi \approx 2$. This value depends on the moment–curvature idealization used to determine the global yield curvature of a wall section. Since the overall drift measured at the top of a wall is considered by most codes as an indicator of the rotational demand at the wall base, note that the largest mean overall drift predicted in this work is about 1.5% for a 5-storey wall and reduces to about 0.6% for a 40-storey wall.

4.1. Influence of wall aspect ratio (A_r)

Figure 6 shows the influence of A_r on dynamic shear amplification and curvature ductility demand for a 10-storey wall with a site class C and $\gamma_w = 2.0$. Based on the OS predictions (Fig. 6*a*), dynamic shear amplification increases with A_r, especially for $T = 1.0$ s. The VT2 predictions (Fig. 6*b*), however, indicate no such significant increase for $T = 1.0$ s, even no increase for $T = 1.5$ s, and much lower amplification values. Although not shown, the profiles of the force demands along the wall height predicted with OS and VT2 are quite similar and do not significantly change with the selected A_r. As shown in Fig. 6*c*, the main influence of A_r is on the base curvature ductility demand, which largely increases with decreasing A_r. For a given A_r value, this ductility demand also increases with T. Note that the predicted plasticity height at the wall base, which is the height from the base over which $\mu_\phi \geq 1$, is about 10% of the wall height (H) irrespective of A_r. This suggests that A_r, and hence the wall length (l_w), has a negligible influence on the plasticity height since the wall height is kept constant. This result, however, has to be balanced with the fact that the plasticity height predictions do not account for inelastic shear deformation and shear cracking, which can produce significantly larger plasticity heights for walls with low A_r values (Bohl and Adebar 2011). The results shown in Figs. 6*b* and 6*c* suggest that there is no relation between the dynamic shear amplification and the curvature ductility demand at the wall base. Furthermore, in general no plastic hinge mechanism is predicted at the upper storeys in spite of light flexural yielding, as illustrated in Fig. 6*c*.

4.2. Influence of site class (SC)

Figure 7 shows the influence of the SC, predicted with VT2, on dynamic shear amplification and shear force demand for wall cases with $N = 5$ and 10 and $\gamma_w = 2.0$. Figures 7*a* and 7*b* show that the selected SC has no significant influence on the AOS dynamic shear amplification, especially for $T \geq 1.0$ s. The dynamic shear amplification at the wall base appears to be more sensitive to the selected SC,

Fig. 6. Influence of wall aspect ratio on seismic response: (*a*) dynamic shear amplification (from OS); (*b*) dynamic shear amplification (from VT2); (*c*) curvature ductility demand (from OS; $\mu_\phi = 1 \equiv$ sectional yielding).

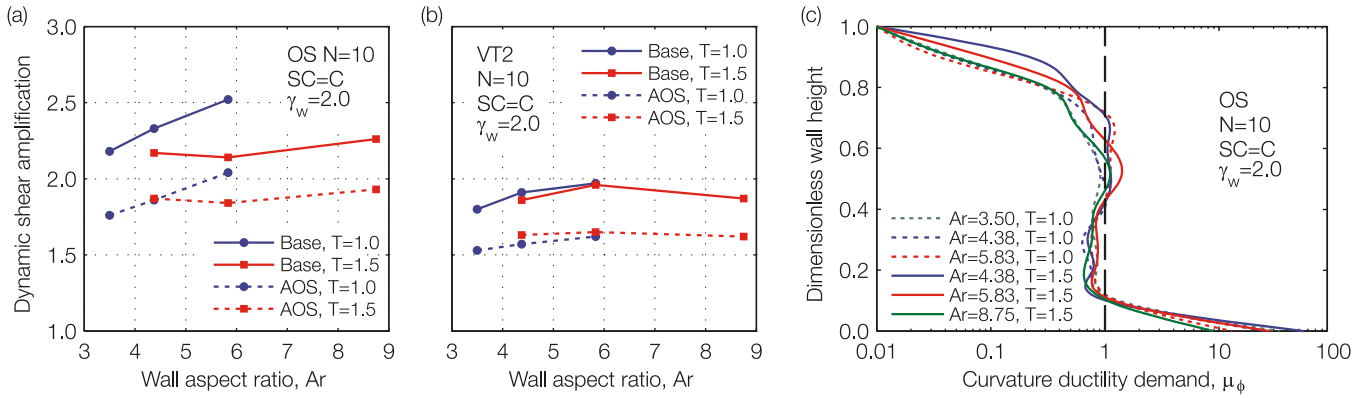

Fig. 7. Influence of site class on seismic response (from VT2): (*a*) dynamic shear amplification for $N = 5$; (*b*) dynamic shear amplification for $N = 10$; (*c*) normalized storey shear force demand for $N = 5$.

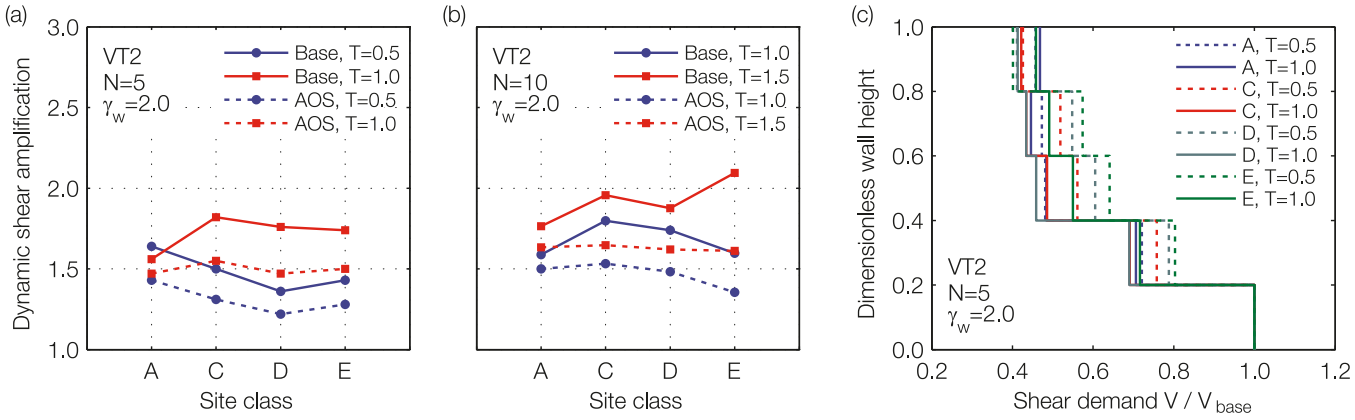

primarily to SCs A and E likely because of their significantly different respective spectrums, as shown in Fig. 2. Although not shown, the OS predictions suggest a much larger sensitivity of dynamic shear amplification to SC. Note that the force demand profiles along the wall height predicted with OS and VT2 are quite similar and do not significantly change with the selected SC, except for the shear force demand predicted with VT2 for $T = 0.5$ s, as illustrated in Fig. 7*c*. Also, in general no plastic hinge mechanism is predicted at the upper storeys for any SC.

4.3. Influence of wall cross-section (WCS)

Figure 8 shows the influence of the WCS, predicted with OS and VT2, on dynamic shear amplification for a 20-storey wall with $T = 2.0$ s, SC = *D*, and $\gamma_w = 2.0$. It is observed that the OS predictions differ significantly in magnitude and trend from the VT2 predictions. The OS predictions suggest that the WCS has no influence on dynamic shear amplification whereas the VT2 predictions indicate a linear decrease of amplification between the WCSs RT and H1, resulting in a base amplification reduction of about 20% between these two WCSs. The dynamic shear amplifications at the wall base predicted with OS for the WCSs RT and H1 are 10% and 40% larger than those predicted with VT2, respectively. This brings up the importance of accounting for nonlinear shear deformation when predicting the seismic shear response of flanged walls. Note that the force demand profiles along

Fig. 8. Influence of wall cross-section on dynamic shear amplification (from OS and VT2).

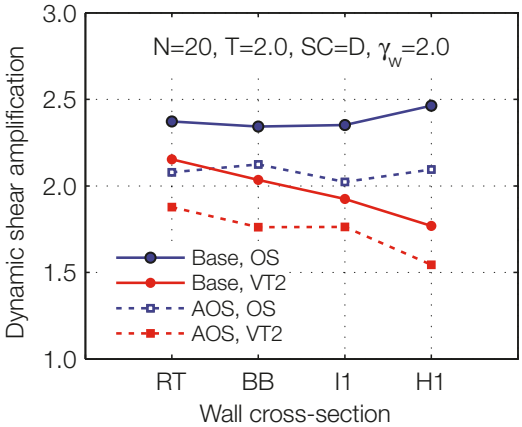

the wall height predicted with OS and VT2 are almost the same and do not significantly change with the selected WCS. Also in general no plastic hinge mechanism is predicted at the upper storeys for any WCS.

4.4. Influence of wall base overstrength (γ_w)

Figure 9 shows the influence of γ_w, predicted with VT2, on dynamic shear amplification and force demand for wall cases with $N = 5$, 10, 15, 20, and 40. The predictions show

Fig. 9. Influence of wall base overstrength (γ_w) on dynamic shear amplification and shear force and moment demands: (*a*) $N = 5$; (*b*) $N = 10$; (*c*) $N = 15$; (*d*) $N = 20$ and 40.

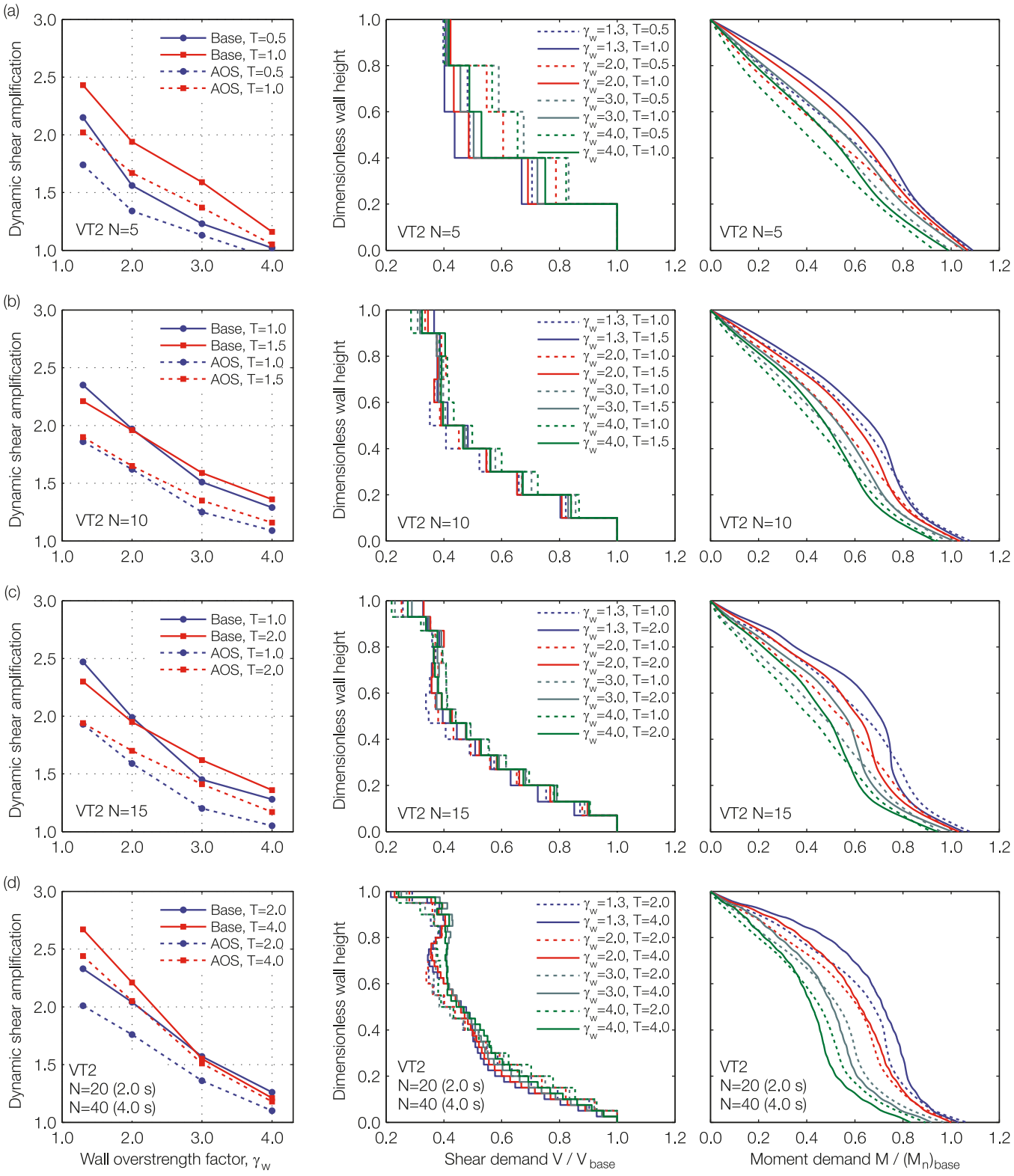

that dynamic shear amplification rapidly decreases, almost linearly sometimes, with increasing γ_w, for any N value. As the γ_w values increase from 1.3 to 4.0, the mean base shear amplification values predicted for all N values decrease from a maximum of 2.7 to a minimum of 1.0. For comparison purposes, the corresponding values predicted with OS are 3.1 and 1.2. The maximum amplification values, which are associated to $T = 4.0$ s and $\gamma_w = 1.3$, predicted with VT2 and OS are by far much lower than the amplification values calculated with ω_v^* (eq. [4]) and ε^* (eq. [7]) for the same T, μ_Δ,

Fig. 10. Influence of wall base overstrength (γ_w) on dynamic shear amplification (from VT2) and comparison with ω_v (eq. [1]).

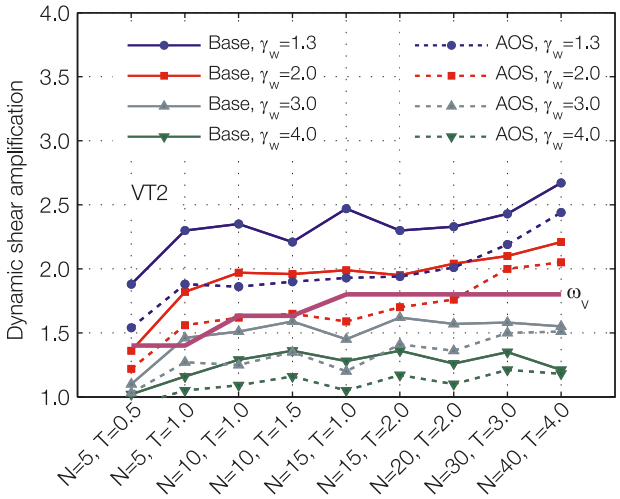

and γ_w values, as observed in Fig. 1. Figure 10, which compares all dynamic shear amplification predictions given in Fig. 9, shows that, for $N = 5$, dynamic shear amplification significantly increases with increasing T from 0.5 s to 1.0 s, and, for the other N values, dynamic shear amplification increases slowly, or reduces sometimes, with increasing N and T. Also this figure shows that ω_v (eq. [1]) conservatively estimates dynamic shear amplification only for $\gamma_w \geq 3.0$. For $\gamma_w = 1.3$, the reductions of base shear amplification observed in Fig. 10 as T increases for a given N result of significant flexural yielding ($\mu_\phi > 2$) at the upper storeys, as illustrated in Fig. 11. Although γ_w affects dynamic shear amplification, Fig. 9 indicates that γ_w has no significant influence on the storey shear force profile along the wall height for $T \geq 1.0$, resulting in very similar profiles.

For the flexural demand, Fig. 9 shows that T and γ_w have a significant influence. Actually as T increases so does the flexural demand, particularly at the upper storeys, but as γ_w increases, this demand reduces rapidly without, however, inhibiting the plastic hinge mechanism at the wall base, even for $\gamma_w = 4.0$, as illustrated in Fig. 11. Curiously, Fig. 11 shows that the curvature ductility demand at the upper storeys for $\gamma_w = 1.3$ and a given T reduces with increasing N. Actually, this reduction results from the required minimum flexural reinforcement which produces at these storeys as N increases, moment resistances increasingly larger than the capacity design moment envelope. Despite this large overstrength, flexural yielding is predicted at the upper storeys, meaning that the flexural demand has significantly exceeded the capacity design envelope. In general, however, no such excess is predicted for $T = 0.5$ s and for $\gamma_w \geq 3.0$ irrespective of T. Figure 11 shows that in general no plastic hinge mechanism is predicted at the upper storeys ($\mu_\phi < 2$) for $\gamma_w \geq 2.0$ despite sometimes light flexural yielding. Figure 9*d* shows a certain match between the moment demand profiles for $T = 2.0$ s and 4.0 s and that the moment profiles associated to $T = 4.0$ s become slightly lower than those associated to $T = 2.0$ s as γ_w increases. Similar observations can be made for curvature ductility demand (see Fig. 11*d*). This suggests that the higher mode contribution to flexural response saturates for $T > 2.0$ s and its relative influence on response becomes less as γ_w increases.

Fig. 11. Influence of wall base overstrength (γ_w) on curvature ductility demand ($\mu_\phi = 1 \equiv$ sectional yielding): (*a*) $N = 5$; (*b*) $N = 10$; (*c*) $N = 15$; (*d*) $N = 20$ and 40.

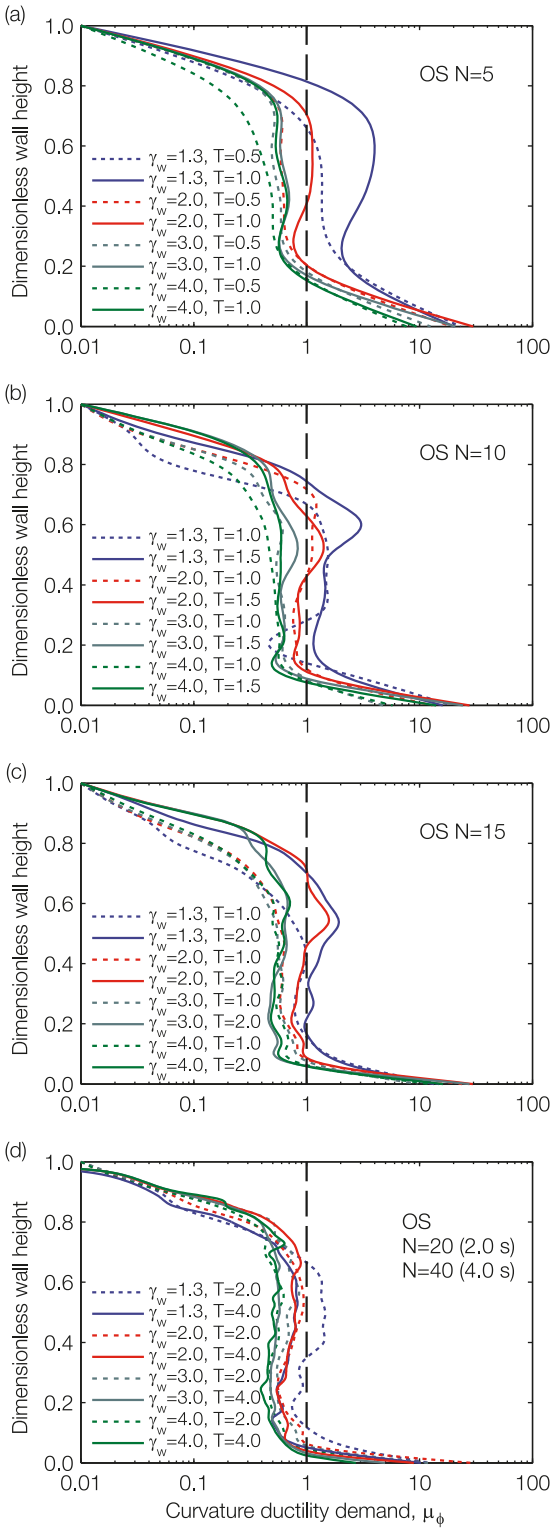

From Fig. 11, note that, for $\gamma_w \geq 2.0$, the plasticity height at the wall base decreases, with respect to H, from about 20% to 2.5% of H as N (or H) and γ_w increase. This differs from the relation $0.5l_w + 0.1H$ prescribed by CSA standard A23.3-04 for determining the base plasticity height requiring special

ductile detailing, where the estimated plasticity height is at least 10% of H and independent of γ_w. This shows that this relation is inadequate, giving too conservative base plasticity height estimates for tall walls with large flexural overstrength at the wall base. Although the plasticity height predictions do not account for inelastic shear deformation and shear cracking, their influence should reduce with increasing H and γ_w, and hence should not change the previous result.

Note that, from all the studied parameters, γ_w has the most significant influence on the dispersion of moment demand predictions but its influence on the dispersion of shear demand predictions is practically negligible, just like that of the other studied parameters. From all the cases considered for studying the influence of γ_w, the coefficient of variation (CV = standard deviation/mean), which is a relative measure of dispersion, for the VT2 moment demand predictions is, on average, about 8% for $\gamma_w = 1.3$ and increases up to about 15% for $\gamma_w = 4.0$, while the CV for the VT2 shear demand predictions is, on average, about 15% for any given γ_w value. This shows that dispersion in force demand predictions is relatively low, in the context of earthquake engineering, and that the lower the γ_w is, or larger the curvature ductility demand is at the wall base, the less scattered are the moment predictions, especially at the wall base where the CV reduces, on average, from about 13% to 3% when γ_w decreases from 4.0 to 1.3, respectively.

5. Discussion

The results presented in the previous sections show that, from the studied parameters, those affecting the most dynamic shear amplification and seismic force demand in ductile RC walls are T and γ_w. Actually they show that, for a given T, the relative higher mode contribution in the seismic force demand highly depends on γ_w. While for any T, dynamic shear amplification largely reduces with increasing γ_w, γ_w has no significant influence on the shear force demand profile for $T \geq 1.0$ s. Moreover, for $T > 1.0$ s, the dynamic shear amplification values slightly increase for $\gamma_w \leq 2.0$ and remain almost constant for $\gamma_w \geq 3.0$, as T increases (see Fig. 10). In general the mean AOS and base shear amplification values predicted with VT2 are much larger than 1.0, with a maximum of 2.7, meaning that the predicted shear force demands have significantly exceeded V_p (eq. [9]), which is the capacity design shear envelope for the plastic hinge zone of wall cases with $\gamma_w < 4.0$. This shows one more time that the capacity design methods prescribed by CSA standard A23.3-04 for shear strength design can produce inadequate design envelopes. In spite of the very large exceeding shear forces, the VT2 predictions showed at worst light shear cracking and light onset of shear reinforcement yielding, even if the shear resistance of each wall case was set to match the capacity design envelope. The recent dynamic test results of Ghorbanirenani (2010) of large-scale 8-storey MD wall specimens designed according to CSA standard A23.3-04 showed stable hysteretic shear responses, no shear reinforcement yielding, and no shear failure of the specimens for base shear demands corresponding up to 150% of the nominal shear resistance (based on the actual material strengths) of the wall or 200% of the design earthquake. These observations suggest that either (*i*) the shear resistance requirements of CSA standard A23.3-04 for MD and ductile shear walls are highly conservative; (*ii*) the energy associated to the high peak shear forces, which are generated by higher mode responses, is not sufficient to sustain the displacement necessary for a shear failure because of the transient nature of these forces and of the unlikelihood that these forces occur simultaneously with the peak displacement responses, which are dominated by the first mode response (Lybas 1981); or (*iii*) a combination of both assumptions. The observations made by Ghorbanirenani (2010) support the first assumption by suggesting a significantly higher contribution of concrete in the base hinge region to shear resistance than that required for design. The predictions obtained in the present work agree with the second assumption because they show that the peak base shear forces and the peak top displacements never occur simultaneously and the base shear forces corresponding to the peak top displacements are generally much lower than the maximum base shear force. The previous assumptions need further investigation but this is beyond the scope of this paper. Meanwhile, the predictions obtained in this work indicate that none of the dynamic shear amplification factors presented in section 2 can adequately estimate, in their current form, the predicted amplification values because their formulation does not generally account for T and γ_w and (or) is not adapted to Canadian seismic provisions. These issues result in estimates that largely differ from those predicted, as observed from Figs. 1 and 10. An adequate general formulation should not only account for T and γ_w but also for the seismic zone and μ_Δ (or $R_d R_o$).

The predictions showed that T and γ_w largely influence the moment demand, which increases with increasing T and reducing γ_w. For $T \geq 1.0$ and $\gamma_w < 3.0$, the predicted flexural demand at the upper storeys has always significantly exceeded the capacity design moment envelope and this excess reduces with increasing γ_w. This shows that the capacity design method prescribed by CSA standard A23.3-04 for flexural strength design can produce inadequate design envelopes. In general, for $\gamma_w \geq 2.0$ and any T, the plastic hinge mechanism is constrained at the wall base, as expected, despite sometimes light flexural yielding at the upper storeys ($\mu_\phi < 2$). This suggests that plastic hinge formation at the upper storeys might be precluded if a minimum γ_w value of 2.0 is forced at the design stage. An additional hinge inhibition would appear when flexural design above the base hinge zone is governed by the required minimum reinforcement, as observed in Fig. 11. It is important to note that these statements only apply to regular wall structures without stiffness and (or) strength irregularities. These irregularities are prone to plastic hinge formation. For instance, preliminary analyses with $\gamma_w = 2.0$ and $T \geq 1.0$ predicted at the upper storeys a plastic hinge at the storey just above a reinforcement curtailment if the wall flexural strength reduction between these two adjacent storeys exceeded about 20% for wall cases with $T = 1.0$ s and about 10% for cases with $T = 4.0$ s (note that no such sensitivity to strength reductions was observed with $\gamma_w \geq 3.0$). Also the 8-storey moderately ductile RC wall specimens ($\gamma_w = 1.145 \equiv 2.29$ for ductile walls, see below) dynamically tested by Ghorbanirenani (2010) with design-level excitations experienced plastic hinge formation at the symmetric setback located just above the wall mid-height. Therefore, all these results suggest that a SPH design may

be inadequate and unsafe for regular ductile cantilever wall structures with $\gamma_w < 2.0$ and for wall structures with stiffness and (or) strength irregularities at the upper storeys. A dual-plastic hinge design (Panagiotou and Restrepo 2009; Ghorbanirenani 2010) may be a better alternative. An additional plastic hinge mechanism located in the upper storeys normally enables a slight reduction of base shear amplification, as shown in Fig. 10 for $\gamma_w = 1.3$.

Note that some of the above results may certainly apply to moderately ductile RC walls designed with CSA standard A23.3-04. For these walls, the product $R_dR_o = 2.0 \times 1.4 = 2.8$, which is half of the total force reduction factor for ductile walls ($R_dR_o = 5.6$). This means that the results obtained for ductile walls with $\gamma_w \geq 2.0$ might theoretically be extended to MD walls with $\gamma_w \geq 1.0$. Using this assumption, Fig. 10 suggests a dynamic base shear amplification value slightly above 1.5 for MD walls with $\gamma_w = 1.3$ ($\equiv 2.6$ for ductile walls). This suggests that CSA standard A23.3-04 should also account for dynamic shear amplification for shear strength design of MD walls, given that the seismic provisions for these walls are much less stringent than for ductile walls. However, the excellent shear performance of the MD wall specimens dynamically tested by Ghorbanirenani (2010) for motion intensities corresponding up to 200% of the design earthquake suggests that it is unnecessary.

6. Conclusion

In this work, a parametric study of regular ductile RC cantilever walls designed with the 2010 NBCC and CSA standard A23.3-04 for Vancouver was performed to investigate the influence of the following parameters on the higher mode amplification effects and hence on the seismic force demand: number of storeys (N), fundamental lateral period (T), site class (SC), wall aspect ratio (A_r), wall cross-section (WCS), and wall base flexural overstrength (γ_w). The study is based on ITHAs, carried out with a large suite of design-level ground motions, of fixed-base isolated walls modelled with two different 2D modeling approaches: a multilayer beam approach (OpenSees) modeling shear deformation linearly and uncoupled to flexure and axial deformations and a smeared membrane element approach (VecTor2) modeling shear deformation inelastically and fully coupled with the flexure–axial interaction. From this study, the following main conclusions can be drawn:

1. Not accounting for inelastic shear deformation and shear–flexure–axial interaction can produce dynamic shear amplification predictions that are much larger in magnitude and inadequate in trend when shear deformation in wall response is significant.
2. The relation $0.5l_w + 0.1H$ prescribed by CSA standard A23.3-04 for determining the base plasticity height requiring special ductile detailing is inadequate, giving too conservative estimates for tall walls with large flexural overstrength at the wall base.
3. The studied parameters affecting the most dynamic shear amplification and seismic force demand are T and γ_w.
4. While for any T, dynamic shear amplification significantly reduces with increasing γ_w, γ_w has no significant influence on the shear force demand profile for $T \geq 1.0$ s. Moreover, for $T > 1.0$ s, dynamic shear amplification slightly increases for $\gamma_w \leq 2.0$ and remains almost constant for $\gamma_w \geq 3.0$, as T increases.
5. None of the reviewed dynamic shear amplification factors can adequately estimate, in their current form, the predicted amplification values because their formulation does not generally account for T and γ_w and (or) is not adapted to Canadian seismic provisions. An adequate general formulation should not only account for T and γ_w but also for the seismic zone and μ_Δ (or R_dR_o).
6. The capacity design methods prescribed by CSA standard A23.3-04 for ductile walls can produce capacity design strength envelopes that fail to conservatively estimate wall shear force demand and to prevent unintended plastic hinge formation at the upper storeys of the wall.
7. A minimum γ_w value of 2.0 can generally preclude the unintended hinge formation at the upper storeys and constrain the plastic mechanism at the wall base, as expected. However, for walls with $2.0 \leq \gamma_w < 3.0$, this observation applies if reinforcement curtailment along the wall height does not result in a flexural strength reduction, between two adjacent storeys, exceeding about 20% to 10% for walls with T_1 ranging from 1.0 s to 4.0 s, respectively.
8. A SPH design may be inadequate and unsafe for regular ductile cantilever wall structures with $\gamma_w < 2.0$ and for wall structures with stiffness and (or) strength irregularities at the upper storeys.

As this work is based on the seismic region of Vancouver, some conclusions may not necessary apply to regions with different seismicity. A similar work is in progress for the eastern Canadian regions.

Acknowledgements

The authors gratefully acknowledge the financial support of the Natural Sciences and Engineering Research Council of Canada (NSERC) for the Canadian Seismic Research Network (CSRN) under the Strategic Research Networks program and of the Fonds de recherche sur la nature et les technologies du Québec (FQRNT), and also the technical support of the Centre for Scientific Computing of the University of Sherbrooke. Computational resources were provided by Calcul Québec and Compute Canada.

References

Adebar, P., and Rad, B.R. 2007. Seismic shear force distribution in high-rise concrete walls. *In* Proceedings of the Ninth Canadian Conference on Earthquake Engineering, Ottawa, Ontario, Canada, 26–29 June 2007, Canadian Association for Earthquake Engineering, pp. 1330–1340.

Aoyama, H. 1987. Earthquake resistant design of reinforced concrete frame buildings with "flexural" walls. Journal of the Faculty of Engineering, **39**(2): 87–109.

Atkinson, G.M. 2009. Earthquake time histories compatible with the 2005 National building code of Canada uniform hazard spectrum. Canadian Journal of Civil Engineering, **36**(6): 991–1000. doi:10.1139/L09-044.

Blakeley, R.W.G., Cooney, R.C., and Megget, L.M. 1975. Seismic shear loading at flexural capacity in cantilever wall structures. Bulletin of the New Zealand National Society for Earthquake Engineering, **8**(4): 278–290.

Bohl, A., and Adebar, P. 2011. Plastic hinge lengths in high-rise concrete shear walls. ACI Structural Journal, **108**(2): 148–157.

Boivin, Y., and Paultre, P. 2010. Seismic performance of a 12-storey ductile concrete shear wall system designed according to the 2005 National building code of Canada and the 2004 Canadian Standard Association standard A23.3. Canadian Journal of Civil Engineering, **37**(1): 1–16. doi:10.1139/L09-115.

Boivin, Y., and Paultre, P. 2012. Seismic force demand on ductile reinforced concrete shear walls subjected to western North American ground motions: Part 2 — new capacity design methods. Canadian Journal of Civil Engineering, **39**(7): 738–750. doi:10.1139/L2012-044.

CAC. 2006. Explanatory notes on CSA standard A23.3-04. Cement Association of Canada (CAC), Ottawa, Ont.

CEN. 2004. Eurocode (EC) 8 - Design of structures for earthquake resistance Part 1: General rules, seismic actions and rules for buildings, EN 1998-1. European Committee for Standardization (CEN), Brussels, Belgium.

Crisp, D.J. 1980. Damping models for inelastic structures. M.E. thesis, Department of Civil Engineering, University of Canterbury, New Zealand.

CSA. 2004. Design of concrete structures. CSA standard A23.3-04 (Update No. 3, August 2009), Canadian Standards Association, Toronto, Ont.

CTBUH. 2008. Recommendations for the seismic design of high-rise buildings. Council on Tall Buildings and Urban Habitat (CTBUH), Chicago, Illinois, USA.

Eberhard, M.O., and Sozen, M.A. 1993. Behavior-based method to determine design shear in earthquake-resistant walls. Journal of Structural Engineering, **119**(2): 619–640. doi:10.1061/(ASCE)0733-9445(1993)119:2(619).

Filiatrault, A., Anderson, D.L., and DeVall, R.H. 1992. Effect of weak foundation on the seismic response of core wall type buildings. Canadian Journal of Civil Engineering, **19**(3): 530–539. doi:10.1139/l92-062.

Filiatrault, A., D'Aronco, D., and Tinawi, R. 1994. Seismic shear demand of ductile cantilever walls: a Canadian code perspective. Canadian Journal of Civil Engineering, **21**(3): 363–376. doi:10.1139/l94-039.

Ghorbanirenani, I. 2010. Experimental and numerical investigations of higher mode effects on seismic inelastic response of reinforced concrete shear walls. Ph.D. thesis, École Polytechnique de Montréal, Département des génies civil, géologique et des mines, Montréal, Que.

Ghosh, S.K., and Markevicius, V.P. 1990. Design of earthquake resistant shearwalls to prevent shear failure. *In* Proceedings of Fourth U.S. National Conference on Earthquake Engineering, Palm Springs, Calif., 20–24 May 1990, Earthquake Engineering Researsh Institute (EERI), Oakland, Calif., Vol. 2, pp. 905–913.

Gilles, D. 2010. In situ dynamic properties of building in Montréal determined from ambient vibration records. Structural Engineering Series Report No. 2010-03, Department of Civil Engineering and Applied Mechanics, McGill University, Montréal, Que.

Goel, R.K., and Chopra, A.K. 1998. Period formulas for concrete shear wall buildings. Journal of Structural Engineering, **124**(4): 426–433. doi:10.1061/(ASCE)0733-9445(1998)124:4(426).

Iqbal, M., and Derecho, A.T. 1980. Inertial forces over height of reinforced concrete structural walls during earthquake. ACI Special Publication - Reinforced Concrete Structures Subjected to Wind and Earthquake Forces, SP-63, pp. 173–196.

Kabeyasawa, T., and Ogata, K. 1984. Ultimate-state design of R/C wall-frame structures. Transactions of the Japan Concrete Institute, **6**: 629–636.

Keintzel, E. 1990. Seismic design shear forces in RC cantilever shear wall structures. European Earthquake Engineering, **3**: 7–16.

Kim, J.Y., Yu, E., Kim, D.Y., and Kim, S.-D. 2009. Calibration of analytical models to assess wind-induced acceleration responses of tall buildings in serviceability level. Engineering Structures, **31**(9): 2086–2096. doi:10.1016/j.engstruct.2009.03.010.

Lee, L.-H., Chang, K.-K., and Chun, Y.-S. 2000. Experimental formulas for the fundamental period of RC buildings with shear-wall dominant systems. Structural Design of Tall Buildings, **9**(4): 295–307. doi:10.1002/1099-1794(200009)9:4<295::AID-TAL153>3.0.CO;2-9.

Léger, P., and Dussault, S. 1992. Seismic-energy dissipation in MDOF structures. Journal of Structural Engineering, **118**(5): 1251–1269. doi:10.1061/(ASCE)0733-9445(1992)118:5(1251).

Linde, P. 1998. Evaluation of structural walls designed according to Eurocode 8 and SIA 160. Earthquake Engineering & Structural Dynamics, **27**(8): 793–809. doi:10.1002/(SICI)1096-9845(199808)27:8<793::AID-EQE756>3.0.CO;2-G.

Lybas, J.M. 1981. Concrete coupled walls: earthquake tests. Journal of the Structural Division, **107**(ST5): 835–855.

Mazzoni, S., McKenna, F., Scott, M.H., and Fenves, G.L. 2006. OpenSees Command Language Manual. Open System for Earthquake Engineering Simulation (OpenSees), Pacific Earthquake Engineering Research (PEER) Center, University of California, Berkeley, California, USA.

Munshi, J.A., and Ghosh, S.K. 2000. Displacement-based seismic design for coupled wall systems. Earthquake Spectra, **16**(3): 621–642. doi:10.1193/1.1586131.

Newmark, N.M., and Hall, W. 1982. Earthquake Spectra and Design. Earthquake Engineering Research Institute, Berkeley, California, USA, 103 p.

NRCC. 2005. National Building Code of Canada; Part 4: Structural Design. Canadian Commission on Building and Fire Codes, National Research Council of Canada (NRCC), Ottawa, Ont.

NRCC. 2010. National Building Code of Canada; Part 4: Structural Design. Canadian Commission on Building and Fire Codes, National Research Council of Canada (NRCC), Ottawa, Ont.

NZS. 2006. NZS 3101 Concrete structures standard, Part 1: The design of concrete structures; Part 2: Commentary on the design of concrete structures. Standards New Zealand, Wellington, New Zealand.

Panagiotou, M., and Restrepo, J.I. 2009. Dual-plastic hinge design concept for reducing higher-mode effects on high-rise cantilever wall buildings. Earthquake Engineering & Structural Dynamics, **38**(12): 1359–1380. doi:10.1002/eqe.905.

Priestley, M.J.N. 2003. Does capacity design do the job? An examination of higher mode effects in cantilever walls. Bulletin of the New Zealand Society for Earthquake Engineering, **36**(4): 276–292.

Priestley, N., and Amaris, A. 2003. Dynamic amplification of seismic moments and shear forces in cantilever walls. *in* Concrete Structures in Seismic Regions, Athens, Greece, Fédération Internationale du Béton (FIB).

Rutenberg, A., and Nsieri, E. 2006. The seismic shear demand in ductile cantilever wall systems and the EC8 provisions. Bulletin of Earthquake Engineering, **4**(1): 1–21. doi:10.1007/s10518-005-5407-9.

Rutenberg, A., and Nsieri, E. 2010. On the seismic shear demand on walls in ductile RC dual systems. *In* Proceedings of the 9th U.S. National and 10th Canadian Conference on Earthquake Engineering, Toronto, Ontario, 25–29 July 2010, Earthquake Engineering Research Institute (EERI), Oakland, Calif.

Sangarayakul, C., and Warnitchai, P. 2004. Approximate modal decomposition of inelastic dynamic responses of wall buildings. Earthquake Engineering & Structural Dynamics, **33**(9): 999–1022. doi:10.1002/eqe.389.

Seneviratna, G.D.P.K., and Krawinkler, H. 1994. Strength and displacement demands for seismic design of structural walls. *In* Proceedings of the 5th US National Conference on Earthquake Engineering, Chicago, Ill., 10–14 July 1994, Earthquake Engineering Research Institute (EERI), Oakland, Calif., Vol. II, pp. 181–190.

Vecchio, F.J. 2000. Disturbed stress field model for reinforced concrete: formulation. Journal of Structural Engineering, **126**(9): 1070–1077. doi:10.1061/(ASCE)0733-9445(2000)126:9(1070).

Ventura, C.E., Lord, J.F., Turek, M., Brincker, R., Andersen, P., and Dascotte, E. 2005. FEM updating of tall buildings using ambient vibration data. *In* Proceedings of the Sixth European Conference on Structural Dynamics (EURODYN), 4–7 September 2005, Paris, France, European Association for Structural Dynamics (EASD), Southampton, United Kingdom. *Edited by* C. Soize and G.I. Schuëller, Millpress, Rotterdam, The Netherlands.

Wong, P.S., and Vecchio, F.J. 2002. VecTor2 and Formworks User's Manual. Civil Engineering, University of Toronto, Toronto, Ont.